ISSN: 1410-8917
e-ISSN: 2597-9914

Jurnal Kimia Sains dan Aplikasi 28 (1) (2025): 47-52

Jurnal Kimia Sains dan Aplikasi
Journal of Scientific and Applied Chemistry

Journal homepage: http://ejournal.undip.ac.id/index.php/ksa

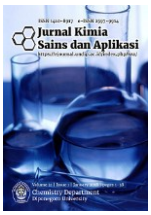

Synthesis and Characterization of Silver Nanoparticles-Chitosan Beads as Antibacterial Agents

Ayu Safirah [1], Atik Rismawati [1], Mohammad Alauhdin [1,*], Sri Wardani [2]

[1] Department of Chemistry, Faculty of Mathematics and Natural Sciences, Universitas Negeri Semarang, Semarang, Indonesia
[2] Department of Chemistry Education, Faculty of Mathematics and Natural Sciences, Universitas Negeri Semarang, Semarang, Indonesia

* Corresponding author: m.alauhdin@mail.unnes.ac.id

https://doi.org/10.14710/jksa.28.1.47-52

Article Info

Article history:

Received: 18th October 2024
Revised: 25th January 2025
Accepted: 30th January 2025
Online: 31st January 2025

Keywords:
beads; characterization; chitosan; silver nanoparticles; synthesis

Abstract

One of the key innovations in silver nanoparticle (AgNPs) material development is the formation of AgNPs/chitosan beads, which exhibit enhanced properties and broader functionality compared to chitosan or AgNPs alone. In this study, AgNPs/chitosan beads were synthesized using glutaraldehyde as a binding agent and sodium citrate as a reducing agent—both of which are safe and non-toxic, enabling broader applications. The synthesized beads were characterized to assess their chemical and physical properties, including functional groups, morphology, and crystallinity. Characterization results confirmed the successful cross-linking of chitosan by glutaraldehyde, enhancing the material's physical and chemical strength. The chitosan beads appeared white, while AgNPs/chitosan beads were brownish, with an average bead size of 1.99 mm. X-ray diffraction analysis revealed that the silver in the chitosan beads exhibited a face-centered cubic crystal structure. Antibacterial testing demonstrated that AgNPs/chitosan beads exhibited superior antibacterial activity compared to chitosan beads, attributed to the release of Ag^+ ions from the matrix.

1. Introduction

Biopolymers are widely utilized as raw materials for various applications due to their desirable properties, such as non-toxicity, biocompatibility, and biodegradability [1, 2]. Among the most studied biopolymers is chitosan, which can be used as solutions, powders, or beads. The $-NH_2$ group in chitosan beads exhibits a higher affinity than chitosan powder, primarily due to diluting weak acids within the chitosan bead matrix, which enhances its adsorption capacity [3, 4]. Additionally, modifying chitosan into bead form can increase its surface area [5]. The hydrophilic nature of the beads further contributes to their common use in drug-delivery systems [1, 6, 7].

Chitosan beads can be synthesized through cross-linking with a polyanionic crosslinking agent, followed by adding NaOH to induce coagulation into bead form [8]. Crosslinking agents are commonly used to enhance the mechanical strength and chemical stability of chitosan beads, particularly in acidic environments. Frequently employed crosslinking agents include sodium tripolyphosphate, epichlorohydrin (ECH), ethylene glycol diglycidyl ether (EGDE), and glutaraldehyde [6, 9, 10]. Chitosan beads cross-linked with glutaraldehyde exhibit reduced swelling and mass loss, improving their structural integrity [11].

A promising innovation in silver nanoparticle (AgNPs) materials is the development of AgNPs/chitosan beads, synthesized by embedding silver within a chitosan hydrogel matrix via silver ion reduction [12, 13, 14]. This material is notable for its antibacterial properties, as chitosan disrupts intracellular bacterial components [6], while AgNPs break down cell walls, interfere with cell synthesis, and inhibit metabolism [15]. The synthesis of chitosan hydrogel/silver nanocomposites using sodium tripolyphosphate as a crosslinking agent and $NaBH_4$ as a reducing agent has demonstrated strong antibacterial activity against *E. coli* and *S. aureus* [16]. However, developing safer, non-toxic reducing agents is essential to align with green chemistry principles.

This article discusses the synthesis and characterization of AgNPs/chitosan beads. The combination of chitosan beads with the unique properties of AgNPs results in a versatile material suitable for various applications, including adsorption [17], antibacterial activity [14, 18, 19], water disinfection [13, 20], drug delivery [16], and wound healing [14, 18, 21]. The synthesis used glutaraldehyde as a safer crosslinker and sodium citrate as a reducing agent, enhancing its applicability. The antibacterial activity was also tested against Gram-positive and Gram-negative bacteria.

2. Experimental

2.1. Materials

The materials used in this study included chitosan (Sigma-Aldrich), acetic acid (CH_3COOH, Merck, 99%), sodium acetate (CH_3COONa, Merck), glutaraldehyde, silver nitrate ($AgNO_3$, Merck), sodium hydroxide (NaOH, Merck), demineralized water, and sodium citrate ($Na_3C_6H_5O_7$, Merck).

2.2. Synthesis of Chitosan Beads

A 2% chitosan solution (10 mL) was mixed with 0.1 mL of 25% glutaraldehyde. The resulting mixture was then loaded into a syringe and dripped slowly into a beaker containing 20 mL of 1.5 M NaOH, where it was left to cure for 24 hours. Once the chitosan beads had formed, they were washed with distilled water until the pH was neutral to remove any residual NaOH.

2.3. Synthesis of AgNPs/Chitosan Beads

The method used was a modification of Yadollahi *et al.* [16] procedure. A 5 mL solution of 2% chitosan was mixed with 10 mL of 3 mM $AgNO_3$ solution, followed by the addition of 0.1 mL of 25% glutaraldehyde. The resulting solution was loaded into a syringe and slowly dripped into a beaker containing a mixture of 10 mL NaOH solution and 10 mL sodium citrate solution, then left to cure for 24 hours. Afterward, the beads were washed with distilled water until the pH was neutral.

2.4. Characterization

The bead size was determined using ImageJ software. Images of the beads were taken with a camera, and the diameters of approximately 100 beads were measured and averaged. Functional groups were analyzed using a Fourier Transform Infrared Spectrophotometer (FTIR, PerkinElmer). The bead samples were dried at room temperature, then ground and mixed with KBr until homogeneous before being pelleted. Measurements were conducted within the wavenumber range of 500–4000 cm^{-1}.

Morphological analysis was performed using Scanning Electron Microscopy (SEM, JEOL JSM-6510LA). The dried beads were sputter-coated, placed on aluminum stubs, and inserted into the sample holder for analysis at an accelerating voltage of 20 kV. The presence of silver nanoparticles in the beads was confirmed by X-ray diffraction (XRD, PANalytical). Diffraction patterns were obtained using Cu-Kα radiation at 40 kV, with a 2θ range of 2–60° and a scan rate of 1°/min.

2.5. Antibacterial Activity

The antibacterial activity of the sample beads was evaluated using the liquid dilution method against Gram-negative *Escherichia coli* (*E. coli*) and Gram-positive *Staphylococcus aureus* (*S. aureus*). Beads were prepared in test tubes at concentrations of 1, 0.1, 0.01, and 0.001 g, each with 1 mL of nutrient broth and 0.1 mL of bacterial suspension. The positive control contained the bacterial suspension, while the negative control had only nutrient broth.

All samples, including the controls, were incubated at 37°C for 24 hours. On the second day, 0.1 mL of each solution was transferred to nutrient agar plates and incubated at 37°C for another 24 hours. Observations were conducted on the third day to assess bacterial growth qualitatively. The presence or absence of bacterial colonies in the nutrient agar indicated antibacterial activity. Increased turbidity and a thicker agar surface suggested higher bacterial growth.

3. Results and Discussion

3.1. Synthesis of Chitosan Beads and AgNPs/Chitosan Beads

Chitosan beads are synthesized by reacting a chitosan solution with glutaraldehyde and dropping the mixture into NaOH to form beads. Glutaraldehyde cross-linking enhances mechanical strength and acid resistance by interacting with chitosan's amine (-NH_2) groups, as seen in Figure 1. The aldehyde groups of glutaraldehyde interact with the protonated amine groups of chitosan via electrostatic forces [17]. Cross-linking improves the chemical stability of chitosan beads; however, it can also reduce the availability of active functional groups. Consequently, this may diminish the material's effectiveness as an adsorbent, antibacterial agent, or other functional application.

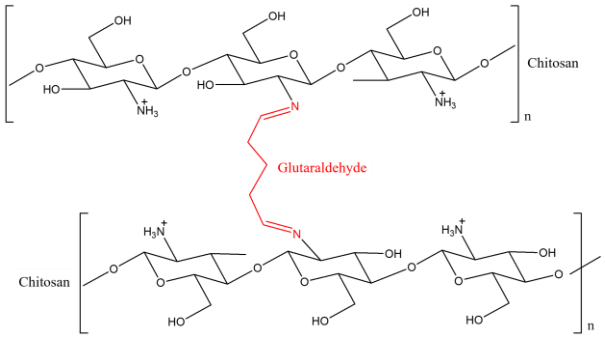

Figure 1. Crosslinking of chitosan by glutaraldehyde through amine groups

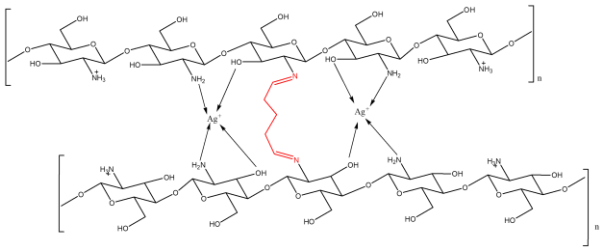

Figure 2. The interaction between Ag^+ ions and the active groups in chitosan

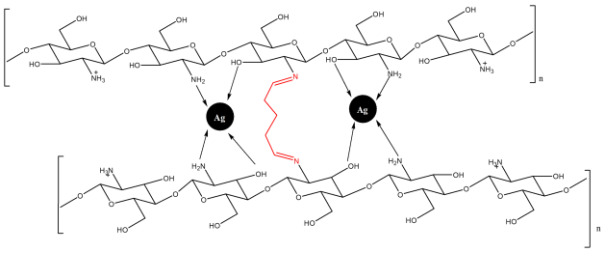

Figure 3. Reduction of Ag^+ ions bound to chitosan into Ag

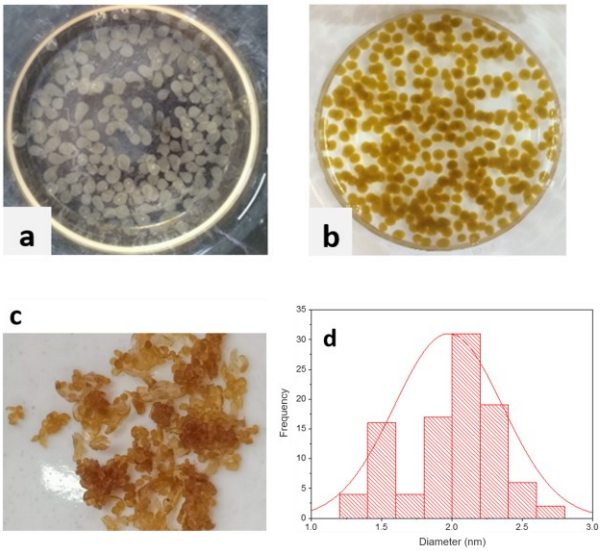

Figure 4. (a) Chitosan beads in NaOH solution, (b) AgNPs/chitosan beads in NaOH solution, (c) dried AgNPs/chitosan beads, and (d) size distribution of wet AgNPs/chitosan beads

Chitosan beads are formed by coagulating a chitosan solution when dropped into a NaOH solution. In an alkaline environment, the chitosan acid solution undergoes a reduction in polymer charge density, leading to the formation of a hydrogel through hydrogen bonding and hydrophobic interactions [22]. The resulting white beads, approximately 2.5 mm in diameter, shrink and become irregular after drying at room temperature.

The synthesis of AgNPs/chitosan beads follows the same procedure as that of chitosan beads, with the key difference being the addition of $AgNO_3$ as a silver nanoparticle precursor and sodium citrate as a reducing agent. While mixing chitosan solution with silver nitrate, Ag^+ ions bind to the amine and hydroxyl groups of chitosan (Figure 2). Bead formation occurs through coagulation, and the Ag^+ ions are subsequently reduced by sodium citrate, forming Ag within the beads (Figure 3).

The formation of silver nanoparticles is indicated by a color change in the beads from white to blackish brown when immersed in a mixture of NaOH and sodium citrate solutions (Figure 4). This color change confirms the reduction of silver ions by sodium citrate. The resulting AgNPs/chitosan beads are spherical, with an average diameter of approximately 1.99 mm in wet conditions, based on measurements of 100 beads (Figure 4). These beads have a smooth surface when hydrated. However, after drying, they shrink, become irregular in shape, and tend to clump together.

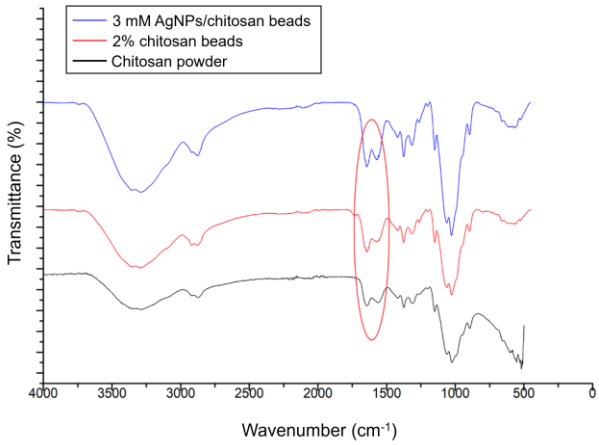

Figure 5. FTIR spectra of chitosan powder, chitosan beads, and AgNPs/chitosan beads

The choice of cross-linking agents influences the final bead size due to variations in molecular size and interactions between the cross-linker and chitosan. Chitosan/Ag nanocomposites synthesized using sodium tripolyphosphate as a cross-linker produce beads ranging from 3 to 4 mm in size [16]. In contrast, using ethylene glycol glycidyl ether (EGDE) results in beads with an average size of approximately 0.53 mm [17].

3.2. Characterization of Beads

The functional groups in the bead samples were analyzed using FTIR and compared with those in chitosan powder (Figure 5). In the FTIR spectra of chitosan, an absorption band at 3290 cm^{-1} corresponds to NH and OH stretching vibrations. Bands at 2918 cm^{-1} and 1376 cm^{-1} arise from -CH stretching vibrations, while the -C=O stretching from amides appears at 1645 cm^{-1}. Additionally, bands at 1568 cm^{-1} and 1315 cm^{-1} are attributed to -NH stretching and -CN bending from the N-acetyl group ($-NHCOCH_3$). The absorption band at 1026 cm^{-1} corresponds to C-O-C stretching, while the 1060 cm^{-1} band originates from asymmetric glucosamine ring stretching.

The FTIR spectra of chitosan and chitosan beads are generally similar, except for the 1540–1560 cm^{-1} region, corresponding to $-NH_2$ bending vibrations. In chitosan beads, the reduced splitting of two peaks in this region (Figure 5, red circle) suggests the transformation of primary amines into secondary amines due to glutaraldehyde crosslinking. This confirms the successful formation of crosslinked chitosan.

Surface morphology plays a crucial role in applying chitosan beads [16]. The incorporation of AgNPs influences the surface morphology of the beads, thereby affecting their properties. SEM images of chitosan beads and AgNPs/chitosan beads are shown in Figure 6. The images do not clearly reveal the bead shape due to coagulation during drying. Additionally, the pores within the beads are not visible in the SEM images, likely because the beads shrink during drying. This shrinkage occurs as solvent molecules are lost from the beads. The empty spaces left by the evaporating solvent molecules could form pores; however, these pores close or fuse together during the drying process.

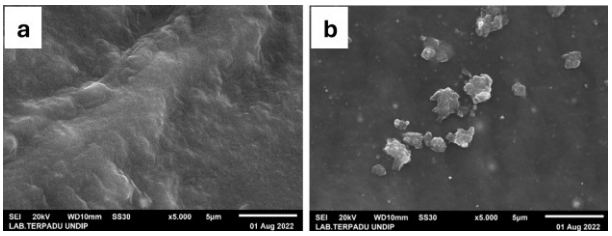

Figure 6. SEM images of (a) chitosan beads and (b) AgNPs/chitosan beads. Scale bar = 5 µm

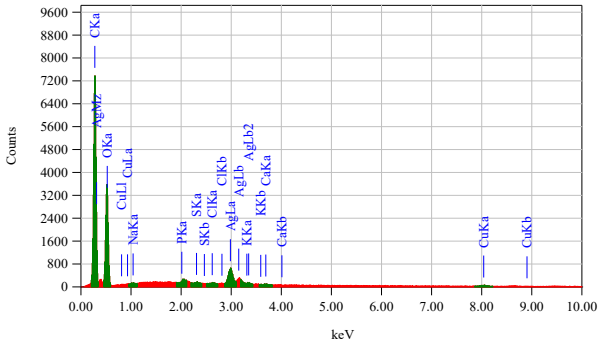

Figure 7. EDX spectra of AgNPs/chitosan beads

The SEM image of AgNPs/chitosan beads shows brighter regions due to the presence of Ag. EDX analysis (Figure 7) confirms the presence of Ag, indicated by a peak at 2.983 keV, corresponding to 2.79% of the total composition. The peak around 3 keV is characteristic of AgNPs, resulting from surface plasmon resonance [23]. This observation confirms that the sodium citrate reductant has successfully reduced Ag^+ ions to Ag^0.

XRD analysis was conducted to determine the presence of Ag in chitosan beads and to identify the formation of Ag crystal planes. The diffractogram (Figure 8) of chitosan beads reveals three diffraction peaks at 2θ values of 20.09°, 27.93°, and 72.40°. The absence of a peak around 2θ 10° suggests low crystallinity of chitosan. While chitosan can be semi-crystalline, the chitosan used in this study appears to be predominantly non-crystalline. The peak at 2θ 20.09° supports this observation, as it is characteristic of hydrated chitosan with a low degree of deacetylation [17].

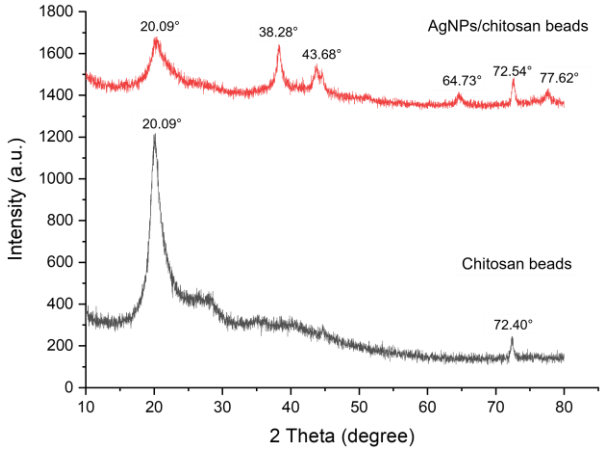

Figure 8. Diffractogram of AgNPs/chitosan beads and chitosan beads

In AgNPs/chitosan beads, the presence of Ag is confirmed by the appearance of characteristic peaks at 2θ values of 38.28°, 43.68°, 64.73°, and 77.62°, corresponding to the planes (111), (200), (220), and (311), respectively. These peaks align with the face-centered cubic (FCC) pattern of Ag and are consistent with data from the Joint Committee of Powder Diffraction Standards (JCPDS) card No. 087-0720. These peaks indicate the formation of metallic silver particles within the beads. The crystallite size of the silver nanoparticles was calculated using the Scherrer equation, yielding an average size of 15.8 nm.

3.3. Antibacterial Activity

The antibacterial activity of the beads was tested against *E. coli* and *S. aureus*. The chitosan bead sample showed bacterial growth on nutrient agar media. In contrast, AgNPs/chitosan beads exhibited no bacterial growth at a bead mass of 1 gram for *S. aureus*. For *E. coli*, three bacterial colonies were still present during repeated tests. Smaller bead mass variations (ranging from 0.001 to 0.1 g) resulted in more bacterial growth for both types of bacteria. These results indicate that AgNPs/chitosan beads exhibit better antibacterial activity than chitosan beads, particularly against *S. aureus*. The observed differences in antibacterial activity between *S. aureus* (a gram-positive bacterium) and *E. coli* (a gram-negative bacterium) can be attributed to the structural differences in their cell walls.

Gram-negative bacteria have cell walls with a multilayer structure, which includes a thin peptidoglycan layer, a lipoprotein layer, phospholipids, and a lipopolysaccharide layer. In contrast, Gram-positive bacteria have a single, thick peptidoglycan layer [24]. The bacterial wall of *S. aureus* consists of only one layer, allowing AgNPs/chitosan to interact more easily with its cell wall than *E. coli*. AgNPs/chitosan beads demonstrate better antibacterial activity than chitosan beads due to the release of Ag^+ ions. AgNPs releases Ag^+ ions upon contact with organic substances [25]. The interaction between Ag^+ ions from AgNPs and the cell walls or cytoplasmic proteins of bacteria, which contain phosphorus or sulfur, leads to metabolic changes that result in bacterial cell death [26].

4. Conclusion

Chitosan beads and AgNPs/chitosan beads were successfully synthesized. The chitosan beads were cloudy white in color and measured approximately 3–6 mm, while the AgNPs/chitosan beads were blackish brown and measured about 2.5 mm. FTIR, SEM, and XRD analysis confirmed the formation of both chitosan beads and AgNPs/chitosan beads. Chitosan beads were formed through the cross-linking of chitosan with glutaraldehyde in the presence of sodium hydroxide. AgNPs was incorporated into the chitosan beads by reducing Ag^+ to Ag^0 by sodium citrate as a reductant. AgNPs/chitosan beads demonstrated superior antibacterial activity compared to chitosan beads, which was attributed to the release of Ag^+ ions within the matrix.

Acknowledgment

This research was funded by DIPA Universitas Negeri Semarang under No. DIPA-023.17.2.677507/2022.

References

[1] Ekhlas A. El-Alfy, Manal K. El-Bisi, Ghada M. Taha, Hassan M. Ibrahim, Preparation of biocompatible chitosan nanoparticles loaded by tetracycline, gentamycin and ciprofloxacin as novel drug delivery system for improvement the antibacterial properties of cellulose based fabrics, *International Journal of Biological Macromolecules*, 161, (2020), 1247-1260 https://doi.org/10.1016/j.ijbiomac.2020.06.118

[2] V. Gopinath, D. MubarakAli, Jamuna Vadivelu, S. Manjunath Kamath, Asad Syed, Abdallah M. Elgorban, Synthesis of biocompatible chitosan decorated silver nanoparticles biocomposites for enhanced antimicrobial and anticancer property, *Process Biochemistry*, 99, (2020), 348-356 https://doi.org/10.1016/j.procbio.2020.09.011

[3] Yuru Yang, Lei Zeng, Zongkun Lin, Huabin Jiang, Aiping Zhang, Adsorption of Pb^{2+}, Cu^{2+} and Cd^{2+} by sulfhydryl modified chitosan beads, *Carbohydrate Polymers*, 274, (2021), 118622 https://doi.org/10.1016/j.carbpol.2021.118622

[4] Zhicong Lan, Yan Lin, Chunping Yang, Lanthanum-iron incorporated chitosan beads for adsorption of phosphate and cadmium from aqueous solutions, *Chemical Engineering Journal*, 448, (2022), 137519 https://doi.org/10.1016/j.cej.2022.137519

[5] Maganda Ananda Kristi, Dwi Indarti, Tri Mulyono, Padsorpsi Cu^{2+} Menggunakan Kitosan Beads Termodifikasi Formaldehida, *Berkala Sainstek*, 5, 2, (2017), 94-97 https://doi.org/10.19184/bst.v5i2.5555

[6] Bai Qu, Yangchao Luo, Chitosan-based hydrogel beads: Preparations, modifications and applications in food and agriculture sectors – A review, *International Journal of Biological Macromolecules*, 152, (2020), 437-448 https://doi.org/10.1016/j.ijbiomac.2020.02.240

[7] Nipun Babu Varukattu, Raju Vivek, Chandrababu Rejeeth, Ramar Thangam, Thondhi Ponraj, Alok Sharma, Soundarapandian Kannan, Nanostructured pH-responsive biocompatible chitosan coated copper oxide nanoparticles: A polymeric smart intracellular delivery system for doxorubicin in breast cancer cells, *Arabian Journal of Chemistry*, 13, 1, (2020), 2276-2286 https://doi.org/10.1016/j.arabjc.2018.04.012

[8] Akash Balakrishnan, Sowmya Appunni, Keerthiga Gopalram, Immobilized TiO_2/chitosan beads for photocatalytic degradation of 2,4-dichlorophenoxyacetic acid, *International Journal of Biological Macromolecules*, 161, (2020), 282-291 https://doi.org/10.1016/j.ijbiomac.2020.05.204

[9] Meng Zhang, Zhi Zhang, Yazhou Peng, Li Feng, Xuhao Li, Chuanliang Zhao, Khan Sarfaraz, Novel cationic polymer modified magnetic chitosan beads for efficient adsorption of heavy metals and dyes over a wide pH range, *International Journal of Biological Macromolecules*, 156, (2020), 289-301 https://doi.org/10.1016/j.ijbiomac.2020.04.020

[10] Paula Mayara Morais da Silva, Natália Gabriele Camparotto, Tauany de Figueiredo Neves, Katherly Tainá Grego Lira, Valmor Roberto Mastelaro, Carolina Siqueira Franco Picone, Patrícia Prediger, Effective removal of basic dye onto sustainable chitosan beads: Batch and fixed-bed column adsorption, beads stability and mechanism, *Sustainable Chemistry and Pharmacy*, 18, (2020), 100348 https://doi.org/10.1016/j.scp.2020.100348

[11] Bagus Rahmat Basuki, I Gusti Made Sanjaya, Sintesis ikat silang kitosan dengan glutaraldehid serta identifikasi gugus fungsi dan derajat deasetilasinya, *Jurnal Ilmu Dasar*, 10, 1, (2009), 93-101

[12] Haoyang Jiang, Gongzheng Zhang, Bo Xu, Xianqi Feng, Quanming Bai, Guoli Yang, Huanjun Li, Thermosensitive antibacterial Ag nanocomposite hydrogels made by a one-step green synthesis strategy, *New Journal of Chemistry*, 40, 8, (2016), 6650-6657 https://doi.org/10.1039/c5nj03608a

[13] Huayong Luo, Juexi Zeng, Mingqi Xu, Qiongfang Tang, Tao Liu, Shuhan Wu, Shiyin Li, Hongwei Rong, Thermo-responsive/anti-biofouling chitosan hydrogel beads in situ decorated with silver nanoparticles for water disinfection, *International Journal of Biological Macromolecules*, 289, (2025), 138872 https://doi.org/10.1016/j.ijbiomac.2024.138872

[14] Yajuan Xie, Xiaozhu Liao, Jingxiang Zhang, Feiwen Yang, Zengjie Fan, Novel chitosan hydrogels reinforced by silver nanoparticles with ultrahigh mechanical and high antibacterial properties for accelerating wound healing, *International Journal of Biological Macromolecules*, 119, (2018), 402-412 https://doi.org/10.1016/j.ijbiomac.2018.07.060

[15] Zihan Liu, Lili Wang, Xiaomin Zhao, Yapei Luo, Keying Zheng, Minghua Wu, Highly effective antibacterial AgNPs@hinokitiol grafted chitosan for construction of durable antibacterial fabrics, *International Journal of Biological Macromolecules*, 209, (2022), 963-971 https://doi.org/10.1016/j.ijbiomac.2022.04.103

[16] Mehdi Yadollahi, Sana Farhoudian, Hassan Namazi, One-pot synthesis of antibacterial chitosan/silver bio-nanocomposite hydrogel beads as drug delivery systems, *International Journal of Biological Macromolecules*, 79, (2015), 37-43 https://doi.org/10.1016/j.ijbiomac.2015.04.032

[17] Merpiseldin Nitsae, Armeida Madjid, Lukman Hakim, Akhmad Sabarudin, Preparation of chitosan beads using tripolyphosphate and ethylene glycol diglycidyl ether as crosslinker for Cr (VI) adsorption, *Chemistry & Chemical Technology*, 10, 1, (2016), 105-114 https://doi.org/10.23939/chcht10.01.105

[18] Tan Dat Nguyen, Thanh Truc Nguyen, Khanh Loan Ly, Anh Hien Tran, Thi Thanh Ngoc Nguyen, Minh Thuy Vo, Hieu Minh Ho, Ngoc Thao Nhi Dang, Van Toi Vo, Dai Hai Nguyen, Thi Thu Hoai Nguyen, Thi Hiep Nguyen, In Vivo Study of the Antibacterial Chitosan/Polyvinyl Alcohol Loaded with Silver Nanoparticle Hydrogel for Wound Healing Applications, *International Journal of Polymer Science*, 2019, 1, (2019), 7382717 https://doi.org/10.1155/2019/7382717

[19] Reem Mahdi Saleh, Omar Mohammed Hassan, Antibacterial, Antibiofilm, and Quorum Quenching Properties of Biogenic Chitosan Silver Nanoparticles Against *Staphylococcus aureus*, *BioNanoScience*, 14, 4,

(2024), 4456-4468
https://doi.org/10.1007/s12668-024-01573-z

[20] Shuhan Wu, Huayong Luo, Shiyin Li, Zexin Zheng, Qingwu Long, Chunhai Wei, Hongwei Rong, Polydopamine/chitosan hydrogels-functionalized polyurethane foams in situ decorated with silver nanoparticles for water disinfection, *Journal of Environmental Management*, 366, (2024), 121858 https://doi.org/10.1016/j.jenvman.2024.121858

[21] Nosheen Masood, Rashid Ahmed, Muhammad Tariq, Zahoor Ahmed, Muhammad Shareef Masoud, Imran Ali, Rehana Asghar, Anisa Andleeb, Anwarul Hasan, Silver nanoparticle impregnated chitosan-PEG hydrogel enhances wound healing in diabetes induced rabbits, *International Journal of Pharmaceutics*, 559, (2019), 23-36 https://doi.org/10.1016/j.ijpharm.2019.01.019

[22] Ecaterina Stela Dragan, Maria Valentina Dinu, Advances in porous chitosan-based composite hydrogels: Synthesis and applications, *Reactive and Functional Polymers*, 146, (2020), 104372 https://doi.org/10.1016/j.reactfunctpolym.2019.104372

[23] Ayşe Baran, Mehmet Fırat Baran, Cumali Keskin, Abdulkerim Hatipoğlu, Ömer Yavuz, Sevgi İrtegün Kandemir, Mehmet Tevfik Adican, Rovshan Khalilov, Afat Mammadova, Elham Ahmadian, Gvozden Rosić, Dragica Selakovic, Aziz Eftekhari, Investigation of Antimicrobial and Cytotoxic Properties and Specification of Silver Nanoparticles (AgNPs) Derived From *Cicer arietinum* L. Green Leaf Extract, *Frontiers in Bioengineering and Biotechnology*, 10, (2022), 855136 https://doi.org/10.3389/fbioe.2022.855136

[24] Muhammad Iqbal Hidayat, Muhammad Adlim, Ilham Maulana, Suhartono Suhartono, Zinatul Hayati, Noor Hana Hanif Abu Bakar, Green synthesis of chitosan-stabilized silver-colloidal nanoparticles immobilized on white-silica-gel beads and the antibacterial activities in a simulated-air-filter, *Arabian Journal of Chemistry*, 15, 2, (2022), 103596 https://doi.org/10.1016/j.arabjc.2021.103596

[25] Toufique Ahmed, R. Tugrul Ogulata, Osman Gülnaz, Recoverable antibacterial property loss of green synthesized AgNPs loaded cotton fabrics with time, *Results in Chemistry*, 4, (2022), 100462 https://doi.org/10.1016/j.rechem.2022.100462

[26] Sukumaran Prabhu, Eldho K. Poulose, Silver nanoparticles: mechanism of antimicrobial action, synthesis, medical applications, and toxicity effects, *International Nano Letters*, 2, (2012), 32 https://doi.org/10.1186/2228-5326-2-32